

Recovery Behavior of the Luminescence Peak from Graphitic Carbon Nitride as a Function of the Synthesis Temperature

Eugene B. Chubenko,* Nikita M. Denisov, Aleksey V. Baglov, Vitaly P. Bondarenko, Vladimir V. Uglov, and Viktor E. Borisenko

Graphitic carbon nitride ($g\text{-C}_3\text{N}_4$) is synthesized by thermal decomposition of thiourea and subsequent in situ polymerization of the products in the oxygen-containing ambient at 450–625 °C and studied with scanning electron microscopy, X-ray diffraction, energy-dispersive X-ray spectroscopy, Fourier-transform infrared spectroscopy, and photoluminescence techniques. The synthesized material contains oxygen at a concentration increasing with the processing temperature from 4.8 to 9.8 at %. The photoluminescence peak is found to be red-shifted with the temperature increased to 575 °C becoming then blue-shifted at higher temperatures. The observed red-shift of the photoluminescence peak is supposed to be caused by band-gap narrowing in $g\text{-C}_3\text{N}_4$ doped by oxygen while its recovery behavior is controlled by thermally induced oxygen-assisted disruption of sp^2 bonds in C-N π -orbital conjugated system of tri-s-triazine units building polymer sheets in $g\text{-C}_3\text{N}_4$.

1. Introduction

Graphitic carbon nitride ($g\text{-C}_3\text{N}_4$) is a polymeric semiconductor with a band gap of 2.7 eV.^[1] Similar to graphite, bulk $g\text{-C}_3\text{N}_4$ has a layered structure. Each layer is composed of tri-s-triazine units connected by tertiary amino groups. Since the layers are connected by weak van-der-Waals forces, they can be easily exfoliated by numerous methods (thermal, ultrasonic, chemical treatment) yielding 2D sheets with larger surface area and band gap compared to those in the bulk material.^[2] The material has attracted the considerable interest of researchers due to its fascinating photocatalytic and luminescent properties combined with the

Dr. E. B. Chubenko, N. M. Denisov, A. V. Baglov, Prof. V. P. Bondarenko, Dr. V. E. Borisenko
Belarusian State University of Informatics and Radioelectronics
P. Browka 6, 220013 Minsk, Belarus
E-mail: eugene.chubenko@bsuir.by

Dr. V. V. Uglov
Belarusian State University
Nezavisimosti Av. 2, 220030 Minsk, Belarus

Dr. V. V. Uglov
South Ural State University
Lenina Av. 76, 454080 Chelyabinsk, Russia

Dr. V. E. Borisenko
National Research Nuclear University MEPhI
Kashirskoe Shosse 31, 115409 Moscow, Russia

 The ORCID identification number(s) for the author(s) of this article can be found under <https://doi.org/10.1002/crat.201900163>

DOI: 10.1002/crat.201900163

simplicity of its synthesis using low-cost nitrogen-rich organic compounds (melamine, cyanamide, dicyandiamide, urea, thiourea) as precursors.^[3]

High-intensity photoluminescence (PL) from $g\text{-C}_3\text{N}_4$ is reproducibly observed at room temperature giving rise to its prospects for light-emitting devices. The position of the PL emission peak of $g\text{-C}_3\text{N}_4$ depends on the synthesis temperature and can be tuned throughout the whole visible spectrum.^[4] Moreover, thermal quenching of the luminescence has been proposed for the use in luminescence-based temperature sensors.^[5] The position of the PL emission peak was noted to demonstrate a monotonous red-shift with an increase

of the polymerization temperature in the range of 300–650 °C when melamine is used as a precursor.^[4] The same trend was observed in case of thiourea used as a precursor while according to the optical absorption measurements, energy band gap of the material reduced from 2.71 to 2.58 eV when the processing temperature was increased from 450 to 550 °C and then increased to 2.76 eV upon processing at 650 °C.^[6]

We have tested this contradiction with thiourea as a precursor. Contrary to the results presented by Zhang et al.^[4] we have observed non-monotonous variation of the PL emission peak with the processing temperature. The experimental results obtained and their discussion is presented in this paper. We choose thiourea because it is a cheap and common commercially available substance suitable as a precursor for large scale $g\text{-C}_3\text{N}_4$ production. In spite of that, to date there are very few studies on the PL properties of thiourea-derived $g\text{-C}_3\text{N}_4$, of which only one^[6] covers the effect of thermal synthesis temperature.

2. Results

Thermal processing of thiourea resulted in the formation of a fragile yellow material with the mass yield decreasing from 15.5% at 450 °C to 8.5% at 575 °C and then to 0.4% at 625 °C.

The typical morphology of the synthesized material is illustrated by the scanning electron microscopy (SEM) image presented in **Figure 1**. It slightly varies with the processing temperature but in general the material consists of multiple layers of plane sheets covered with small flat flakes and particles of different sizes ranging from several micrometers to 20 nm.

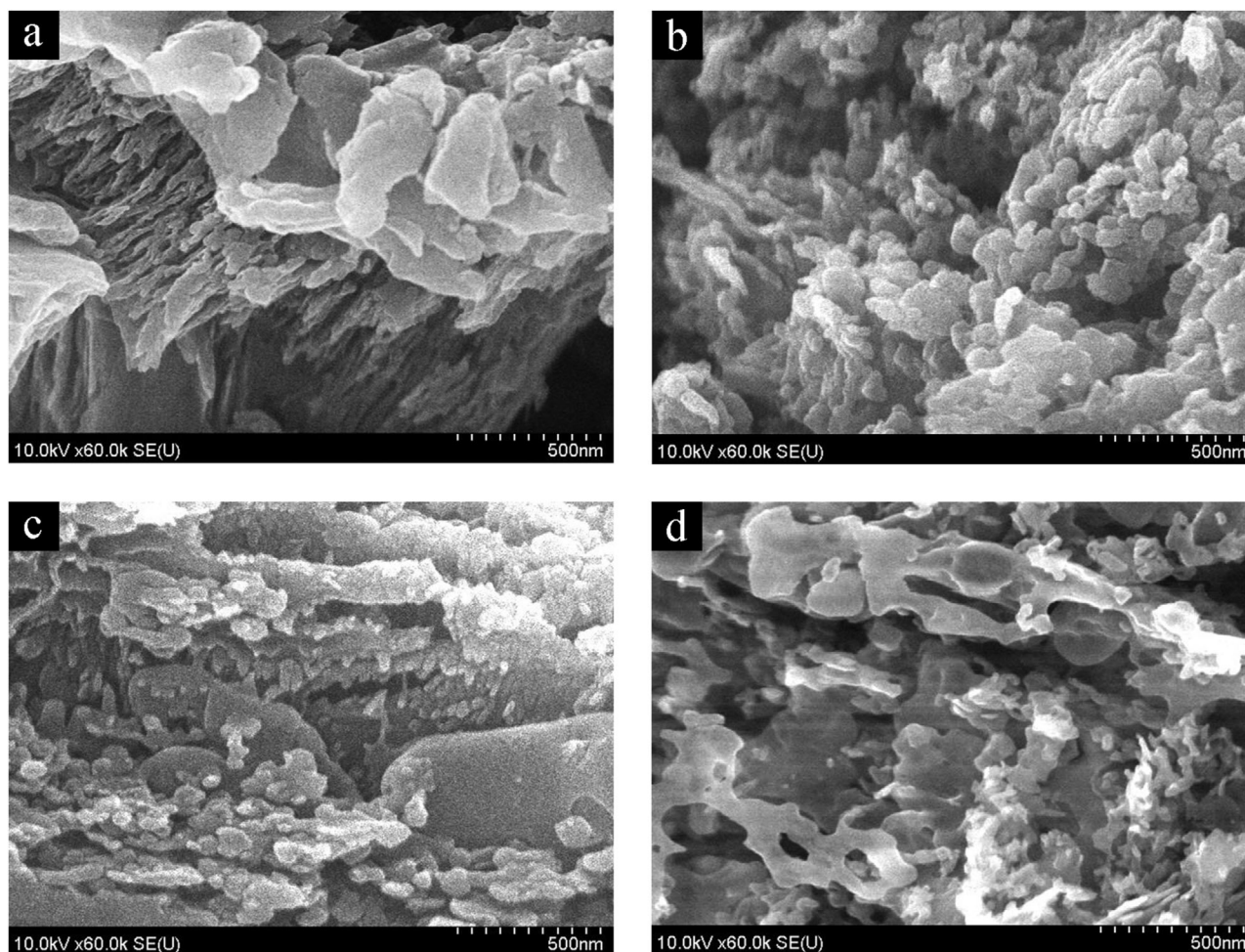


Figure 1. SEM image of the material synthesized at different temperatures: a) 450 °C, b) 500 °C, c) 550 °C, d) 600 °C.

Table 1. Content of the elements in the synthesized material.

Synthesis temperature [°C]	Content of an element [at%]			C/N ratio
	C	N	O	
450	32.12	63.10	4.78	0.509
500	32.29	62.75	4.96	0.514
550	32.27	60.23	7.50	0.536
600	34.77	55.47	9.76	0.627

The composition of the material estimated with the energy-dispersive X-ray spectroscopy (EDX) analysis is represented by three main elements which are carbon, nitrogen, and oxygen. Their content as a function of the processing temperature is summarized in **Table 1**.

The content of carbon (C) slightly increases (by 2.65 %) with the synthesis temperature, while the decrease in nitrogen (N) content (by 7.63 %) and the twofold increase in oxygen (O) content are observed for the temperature range 450–600 °C. At the same time, the C/N ratio gradually increases from 0.509 (at

450 °C) to 0.536 (at 550 °C), followed by the abrupt increase to 0.627 (at 600 °C).

The X-ray diffraction (XRD) analysis demonstrated that crystalline C_3N_4 polymer material was synthesized. It is illustrated by the spectra shown in **Figure 2**. Characteristic bands at 12.95–13.25 deg and 27.55–27.90 deg associated with (210) and (002) phases of $g-C_3N_4$ with widely accepted tri-s-triazine structure^[8] are observed. Also, a low-intensity band at 57.75 deg corresponding to (004) $g-C_3N_4$ can be resolved.

The position of the most prominent (002) XRD peak is slightly shifted to larger 2θ angles with the increase of the processing temperature (see **Table 2**). This peak is associated with stacking of aromatic units in tri-s-triazine $g-C_3N_4$ structure.^[9,10] The peak position corresponds to interplanar distance between aromatic ring units. The calculated distance $d_{(002)}$ decreases with the temperature from 3.23 to 3.195 Å upon processing at 500 to 600 °C, respectively. They are significantly smaller than those theoretically calculated for ideal crystalline $g-C_3N_4$ tri-s-triazine units with layer-to-layer distance 3.40 Å.^[11]

The position of the peak usually assigned as (210) plane and corresponding to in-plane distance between tri-s-triazine units^[9,10] also slightly shifts with the temperature to larger 2θ angles as well as the distance $d_{(210)}$. In an ideal $g-C_3N_4$ crystal, it has

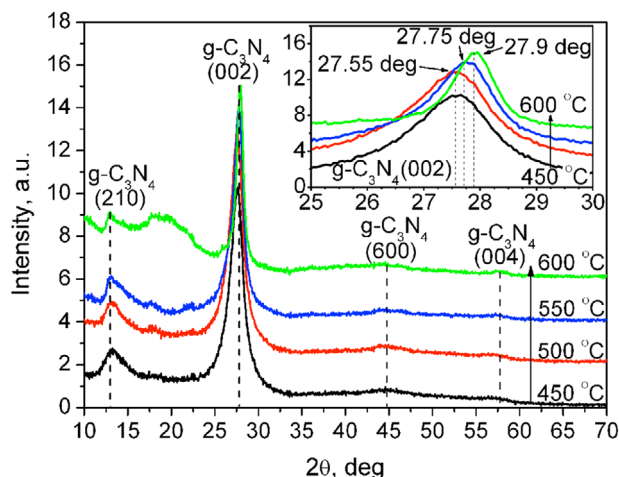


Figure 2. XRD spectra of the materials synthesized from thiourea at different temperatures.

Table 2. XRD peak positions and interplanar distances.

Synthesis temperature [°C]	Position of (002) peak [deg]	Distance $d_{(002)}$ [Å]	Position of (210) peak [deg]	Distance $d_{(210)}$ [Å]	Crystallites size [nm]
450	27.60	3.229	12.95	6.831	43
500	27.55	3.235	13.10	6.753	45
550	27.75	3.212	13.20	6.702	56
600	27.90	3.195	13.25	6.677	84

to be 7.30 Å while 6.68–6.83 Å has been derived from the experimental XRD spectra. It is also admitted that the size of crystallites calculated from the XRD data with Scherrer equation increases with the synthesis temperature (Table 2, last column).

Fourier-transform infrared spectroscopy (FT-IR) spectra of the experimental samples shown in Figure 3 also confirm formation of $g\text{-C}_3\text{N}_4$. Broad band near 3000 cm^{-1} contains at least three absorption lines at 3081, 3168, and 3250 cm^{-1} which represent NH , NH_2 groups and their intermolecular hydrogen bonding.^[11,12] Lines at 2360 and 2340 cm^{-1} are related to gaseous CO_2 ^[13] adsorbed from the atmosphere during the recording of the FT-IR spectra because splitting of the mode is due to coupling with rotational energy modes and not presented on solid or adsorbed CO_2 . Weak line at 2162 cm^{-1} associated with tri-bond cyano groups $\text{C}\equiv\text{N}$ ^[14,15] in the synthesized material is usually attributed to incomplete polymerization of the precursor.^[15] Bands at 1680 and at 1630 cm^{-1} correspond to double $\text{C}=\text{N}$ bond stretching modes^[12,16]; however, 1630 cm^{-1} can also overlap with NH_2 group deformation mode.^[12] The band near 1569 cm^{-1} is a double ring quadrant stretch mode.^[12] Group of adsorption lines near $1400\text{--}1450\text{ cm}^{-1}$ (1454 , 1428 , and 1397 cm^{-1}) is a tri-s-triazine aromatic rings double bond $\text{C}=\text{N}$ stretching modes.^[12,17] The peaks in the $1000\text{--}1350\text{ cm}^{-1}$ (1133 , 1231 , and 1315 cm^{-1}) region can be related to the $\text{C}\text{--}\text{N}$ bonds stretching.^[17] The strong band observed at 1315 cm^{-1} characterizes the $\text{C}\text{--}\text{N}$ stretch in the threefold N-bridge linking the tri-s-triazine rings.^[12] Adsorption with the maximum at 805 cm^{-1} is an out-of-plane ring bending by sextants.^[1,12] Low-intensity absorption bands located at 1081

and 1205 cm^{-1} can be associated with $\text{C}\text{--}\text{O}$ bonds in $g\text{-C}_3\text{N}_4$ structure.^[18,19]

It should be noted that some adsorption lines at the FT-IR spectra shift with the synthesis temperature. For example, the line at 805 cm^{-1} in the $g\text{-C}_3\text{N}_4$ synthesized at 450 °C shifted to 809 cm^{-1} in the material synthesized at 600 °C . The observed changes can be attributed to distortions of crystal lattice of the synthesized $g\text{-C}_3\text{N}_4$.^[12]

PL spectra of the synthesized materials are displayed in Figure 4. The emission peaks at $467\text{--}502\text{ nm}$ become weaker and broader as the processing temperature increases.

The wavelength position of the PL peak intensity demonstrates a recovery behavior illustrated in the inset of Figure 4. It red-shifts from 467 to 502 nm with the processing temperature increasing from 450 to 550 °C , and then blue-shifts to 481 nm with further temperature increase to 625 °C . Full width at half maximum (FWHM) of the PL bands constantly increase with the synthesis temperature from 118.6 nm at 450 °C to 150.4 nm at 625 °C .

3. Discussion

Using thiourea as a precursor, we obtained a relatively high yield of $g\text{-C}_3\text{N}_4$ ($8.45\text{--}15.5\%$) as compared to the earlier reported 6% .^[20] As the synthesis temperature increases, the yield decreases due to combustion and decomposition of thiourea and products of its polymerization.

Despite the synthesized materials demonstrating IR absorption peaks characteristic of $g\text{-C}_3\text{N}_4$, the C/N ratios for all of the samples are below its stoichiometric value of 0.75 (see Table 1). The excess of N atoms can be attributed to incomplete condensation of the products of thiourea decomposition into $g\text{-C}_3\text{N}_4$, so that their certain amount still has amine functional groups^[21,22] (polymeric melem, e.g., contains up to 62.5% of $\text{N}^{[20]}$). The presence of amine groups is supported by the results of FT-IR studies, which found $\text{N}\text{--}\text{H}$ bonds. Incomplete polymerization is typical for $g\text{-C}_3\text{N}_4$ materials synthesized by pyrolytical decomposition and subsequent polymerization of N-rich organic precursors.^[1,9] Thus, the observed N content decrease at high synthesis temperatures is likely to be caused by the increased polymerization degree of the produced materials. It also was confirmed by XRD data, as calculated $g\text{-C}_3\text{N}_4$ crystallites size increases with the synthesis temperature. Considering that O content increases with the synthesis temperature, the decrease in N content may also be attributed to O-doping, since it has been reported to preferentially occur via substitution of N atoms in the lattice of $g\text{-C}_3\text{N}_4$.^[9] Moreover, some of the small peaks at FT-IR spectra arise as synthesis temperature grows (Figure 3) possibly related to $\text{C}\text{--}\text{O}$ bonds.^[18,19] According to Fu et al.,^[14] O-doping can occur during the thermal treatment of already formed $g\text{-C}_3\text{N}_4$ in air, while the highest reported doping level is $10\text{ at}\%$.^[15] We have achieved such oxygen concentration by in situ doping of $g\text{-C}_3\text{N}_4$ during its synthesis. Observed shift of $g\text{-C}_3\text{N}_4$ peaks on XRD spectra to higher 2θ angles as well as shifts of some adsorption lines at the FT-IR spectra points to densification^[11] of the crystal structure with increased synthesis temperature, regardless of the increasing polymerization degree. Increased high O content may be responsible for the observed distortions of $g\text{-C}_3\text{N}_4$ crystal lattice.

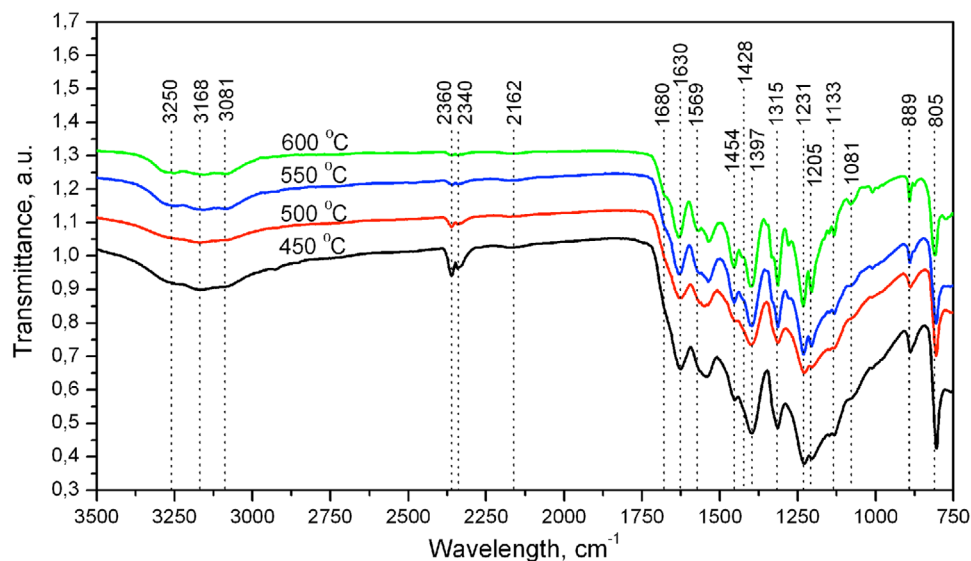


Figure 3. FT-IR spectra of the $g\text{-C}_3\text{N}_4$ synthesized from thiourea at different temperatures.

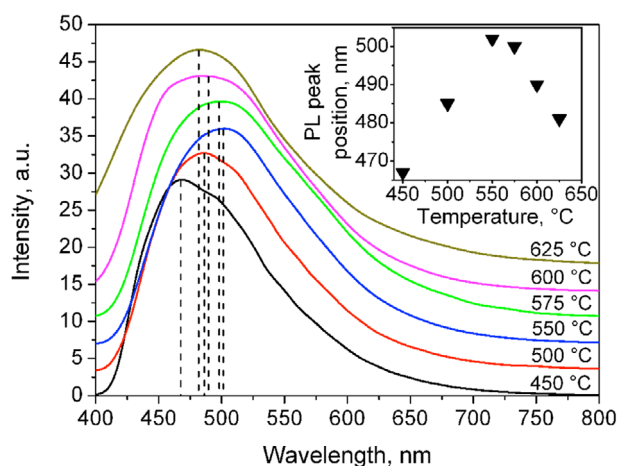


Figure 4. PL spectra and positions of the peak intensity (inset) for the materials synthesized from thiourea at different temperatures. All spectra were normalized by peak intensity and shifted from each other along the “Intensity” axis to better visibility.

PL of $g\text{-C}_3\text{N}_4$ has been interpreted in several studies. According to Yuan et al.,^[20] it is a result of electronic transitions between energy bands formed by sp^3 C-N σ -orbitals, sp^2 C-N π -orbitals, and the lone pair (LP) orbitals of N atom. The excited σ^* - and π^* -orbitals (σ^* and π^* , respectively) form the conduction band, while the σ -, C-N-, and LP-orbitals form the valence band.^[5] The allowed radiative recombination processes include $\sigma^*\text{-LP}$ ($\lambda = 405$ nm), $\pi^*\text{-LP}$ ($\lambda = 480$ nm), and $\pi^*\text{-}\pi$ transitions.^[5]

A decrease of the PL intensity from $g\text{-C}_3\text{N}_4$ synthesized at high temperatures (>575 °C) is usually related to the formation of structure defects, which can capture charge carriers and cause the increased non-radiative recombination rates and shorter lifetime of the carriers.^[2,23–27] Here, PL quenching presumably caused by in situ O-doping of $g\text{-C}_3\text{N}_4$ facilitates charge separation.^[14,18,28,29]

Broadening of the PL peaks with the synthesis temperature increase has been previously ascribed to the increasing degree of $g\text{-C}_3\text{N}_4$ polymerization,^[5,30] increasing disorder in its structure,^[5,30] and impurities (products of $g\text{-C}_3\text{N}_4$ combustion/decomposition).^[20] Results of XRD, EDX, and FT-IR analysis suggest that the polymerization degree and concentration of O atoms increase with the synthesis temperature. The latter can cause the distortion of $g\text{-C}_3\text{N}_4$ crystal lattice also contributing to a broadening of PL peaks.

We have found only one paper by Jourshabani et al.^[31] on the recovery behavior of the PL peak position, which occurred in the synthesis temperature range of 500–584 °C. However, in that study SiO_2 nanoparticles were used as templates in the $g\text{-C}_3\text{N}_4$ synthesis procedure, so the direct comparison of our results is complicated. In a more similar study on thiourea thermal polymerization at 450–650 °C,^[6] a continuous red-shift of the PL peak was observed, despite the recovery behavior of the absorption edge demonstrated by $g\text{-C}_3\text{N}_4$ synthesized at 650 °C.

It is known that two processes, which take place simultaneously during the synthesis of $g\text{-C}_3\text{N}_4$ may show opposite effects on its structure, defect content, and as a result, the PL properties. On the one hand, the increasing degree of $g\text{-C}_3\text{N}_4$ polymerization causes the red-shift of the PL maximum.^[3,20,30] As the amount of connected tri-s-triazine units increases, the π -conjugated system is enhanced, which causes σ^* - and π^* -bands to overlap. This allows relaxation of electrons from σ^* - to π^* -band, so, basically, the band gap of $g\text{-C}_3\text{N}_4$ decreases. Also the red-shift of PL can be the effect of O-doping, since impurities can create levels allowed for radiative recombination.^[17,26,32] The red-shift mechanisms described above can occur simultaneously and cause PL band blurring and broadening because the observed PL spectra can be defined by both of them. On the other hand, keeping already synthesized $g\text{-C}_3\text{N}_4$ at high temperature initiates its combustion, thermal decomposition, and thermal exfoliation. The O concentration in the synthesized $g\text{-C}_3\text{N}_4$ above the certain value also can lead to exfoliation of $g\text{-C}_3\text{N}_4$ layers.^[14] These processes increase

disorder in the material structure, increase the porosity, and thus cause the blue-shift of the PL peak due to either quantum confinement effect^[2,27,33] or disruption of the π -conjugated system. However, the quantum confinement is less probable since the g - C_3N_4 peaks on XRD spectra became narrower with the synthesis temperature growth (Figure 2). The latter mechanism looks more probable in the explanation of the PL blue-shift observed in our experiments.

We suggest that the rate of both competitive processes increases with the synthesis temperature, but above 550 °C, the combustion/decomposition/exfoliation processes overpower the polymerization process, which causes the observed recovery behavior of the PL peak. Considering that either red- or blue-shift were observed in most of the previous studies, the combined phenomenon of the red-shift being replaced by the blue-shift at a certain synthesis temperature is likely to require certain conditions in order to become possible.

4. Conclusions

We have demonstrated that thermal decomposition of thiourea and subsequent polymerization of the products at 450–625 °C in closed oxygen-containing ambient can be used to synthesize g - C_3N_4 in situ doped with oxygen to a concentration up to 9.8 at% at 600 °C. Simultaneously, nitrogen content drops and C/N ratio increases tending to the stoichiometric value of 0.75. Higher processing temperature in the above range promotes better polymerization of g - C_3N_4 , while high concentration of oxygen atoms leads to distortion of its crystalline structure as it is manifested by the shift of (002) g - C_3N_4 peak at XRD spectra. The observed recovery behavior of the PL band of this material as a function of the synthesis temperature is supposed to be defined by two competitive processes. The first one, leading to the red-shift, is associated with band-gap narrowing caused by overlapping of σ^* and π^* energy bands of g - C_3N_4 and corresponding relaxation of electrons from σ^* - to π^* -bands, and caused by growing role of radiative transitions through increasing number of shallow levels in the band gap associated with oxygen atoms. The second process leads to the blue-shift caused by disruption of the sp^2 C-N π -orbital conjugated system in g - C_3N_4 band structure due to combustion, decomposition, exfoliation, and O over-doping of g - C_3N_4 at high synthesis temperatures. The latter process prevails at temperatures above 550 °C. The observed recovery phenomena can be used for fine tuning of the PL peak position according to requirements of particular optoelectronic applications.

5. Experimental Section

Bulk g - C_3N_4 was synthesized by thermal processing of thiourea in a closed air ambient as it was described elsewhere.^[7] A portion of 2 g of this precursor of analytical grade was placed into a porcelain crucible which was then hermetically closed and subjected to thermal processing in a muffle furnace at different temperatures from 450 to 625 °C for 4 h. The heating rate was 5 °C min^{-1} . Cooling was gradual and lasted for 12 h.

The morphology of the synthesized material was investigated by SEM using Hitachi S-4800 apparatus. Its atomic composition was analyzed by EDX using Bruker QUANTAX 200 EDX spectrometer. Crystalline phases in the samples were identified by XRD analysis using DRON-4 diffractometer

($\lambda = 1.54184 \text{ \AA}$). For XRD measurements, the synthesized material was mechanically grinded up to a fine powder and fixed with polyvinylbutyral-based resin on a glass substrate. Chemical bonds in the material were studied with FT-IR using Bruker Vertex 70 FT-IR spectrometer.

Photoluminescence of the material was excited with a monochromatic light of a wavelength of 345 nm, which was cut off from the emission spectra of a 1 kW Xe lamp using a Solar TII DM 160 double monochromator. The emission spectrum was registered by Solar TII MS 7504i monochromator-spectrograph equipped with a Peltier-cooled Hamamatsu S7031-1006S silicon CCD matrix as a detector. Photoluminescence measurements were carried out at 20 °C.

Acknowledgements

This work was supported through the Project 1.56 of the Belarus Government Research Program “Physical materials science, novel materials, and technologies” and by a doctorate grant of the Ministry of Education of the Republic of Belarus. The authors are grateful to D.V. Zhigulin for the SEM and EDX analysis of the samples, and S.M. Zavadski for FT-IR spectroscopy.

Conflict of Interest

The authors declare no conflict of interest.

Keywords

Fourier-transform infrared spectroscopy, graphitic carbon nitride, oxygen doping, photoluminescence, X-ray diffractometry

Received: August 19, 2019

Revised: November 8, 2019

Published online:

- [1] J. Wen, J. Xie, X. Chen, X. Li, *Appl. Surf. Sci.* **2017**, 391, 72.
- [2] F. Dong, Y. Li, Z. Wang, W. K. Ho, *Appl. Surf. Sci.* **2015**, 358, 393.
- [3] A. Sudhaik, P. Raizada, P. Shandilya, D.-Y. Jeong, J.-H. Lim, P. Singh, *J. Ind. Eng. Chem.* **2018**, 67, 28.
- [4] Y. Zhang, Q. Pan, G. Chai, M. Liang, G. Dong, Q. Zhang, J. Qiu, *Sci. Rep.* **2013**, 3, 1943.
- [5] D. Das, S. L. Shinde, K. K. Nanda, *ACS Appl. Mater. Interfaces* **2016**, 8, 2181.
- [6] G. Zhang, J. Zhang, M. Zhang, X. Wang, *J. Mater. Chem.* **2012**, 22, 8083.
- [7] N. M. Denisov, E. B. Chubenko, V. P. Bondarenko, V. E. Borisenko, *Tech. Phys. Lett.* **2019**, 45, 108.
- [8] Y. Zhang, R. Wen, D. Guo, H. Guo, J. Chen, Z. Zheng, *Appl. Organomet. Chem.* **2016**, 30, 160.
- [9] F. Fina, S. K. Callear, G. M. Carins, J. T. S. Irvine, *Chem. Mater.* **2015**, 27, 2612.
- [10] S.C. Yan, Z. S. Li, Z. G. Zou, *Langmuir* **2009**, 25, 10397.
- [11] M. J. Bojdys, J.-O. Miller, M. Antonietti, A. Thomas, *Chem. Eur. J.* **2008**, 14, 8177.
- [12] V. N. Khabashesku, J. L. Zimmerman, J. L. Margrave, *Chem. Mater.* **2000**, 12, 3264.
- [13] G. Lefèvre, T. Preočanin, J. Lützenkirchen, in *Infrared Spectroscopy—Materials Science, Engineering and Technology* (Ed: T. Theophile), IntechOpen, London **2012**, pp. 97–122.

- [14] J. Fu, B. Zhu, C. Jiang, B. Cheng, W. You, J. Yu, *Small* **2017**, *13*, 1603938.
- [15] Y. Li, F. Wei, Y. Liu, H. Zhao, X.-N. Ren, J. Liu, T. Hasan, L. Chen, B.-L. Su, *Nanoscale* **2018**, *10*, 4515.
- [16] M. Zhang, Y. Nakayama, *J. Appl. Phys.* **1997**, *82*, 4912.
- [17] J.L. Zimmerman, R. Williams, V. N. Khabashesku, J. L. Margrave, *Nano Lett.* **2001**, *1*, 731.
- [18] X. Qu, S. Hu, J. Bai, P. Li, G. Lu, X. Kang, *New J. Chem.* **2018**, *2*, 4998.
- [19] Y. Zeng, X. Liu, C. Liu, L. Wang, Y. Xia, S. Zhang, S. Luo, Y. Pei, *Appl. Catal. B Environ.* **2018**, *224*, 1.
- [20] Y. Yuan, L. Zhang, J. Xing, M. I. B. Utama, X. Lu, K. Du, Y. Li, X. Hu, S. Wang, A. Genç, R. Dunin-Borkowski, J. Arbiol, Q. Xiong, *Nanoscale* **2015**, *7*, 12343.
- [21] W. J. Ong, L. L. Tan, Y. H. Ng, S. T. Yong, S. P. Chai, *Chem. Rev.* **2016**, *116*, 7159.
- [22] L. Shi, L. Liang, F. Wang, M. Liu, K. Chen, K. Sun, N. Zhang, *J. Sun. ACS Sustain. Chem. Eng.* **2015**, *3*, 3412.
- [23] P. Wu, J. Wang, J. Zhao, L. Guo, F. E. Osterloh, *J. Mater. Chem. A* **2014**, *2*, 20338.
- [24] F. Dong, Z. Zhao, T. Xiong, Z. Ni, W. Zhang, Y. Sun, W.-K. Ho, *ACS Appl. Mater. Interfaces* **2013**, *5*, 11392.
- [25] Y. Wang, M. Qiao, J. Lv, G. Xu, Z. Zheng, X. Zhang, Y. Wu, *Fullerenes, Nanotubes, Carbon Nanostruct.* **2018**, *26*, 210.
- [26] Z. Wang, W. Guan, Y. Sun, F. Dong, Y. Zhou, W.-K. Ho, *Nanoscale* **2015**, *7*, 2471.
- [27] Z. Zhao, Y. Sun, Q. Luo, F. Dong, H. Li, W.K. Ho, *Sci. Rep.* **2015**, *5*, 14643.
- [28] L.J. Fang, X.L. Wang, J.J. Zhao, Y.H. Li, Y.L. Wang, X.L. Du, Z.F. He, H.D. Zeng, H.G. Yang, *Chem. Commun.* **2016**, *52*, 14408.
- [29] J. Li, B. Shen, Z. Hong, B. Lin, B. Gao, Y. Chen, *Chem. Commun.* **2012**, *48*, 12017.
- [30] H. Zhang, A. Yu, H. Zhang, A. Yu, *J. Phys. Chem. C* **2014**, *118*, 11628.
- [31] M. Jourshabani, Z. Shariatinia, A. Badiei, *Langmuir* **2017**, *33*, 7062.
- [32] G. Dong, D. L. Jacobs, L. Zang, C. Wang, *Appl. Catal. B Environ.* **2017**, *218*, 515.
- [33] J. Xu, Y. Wang, Y. Zhu, *Langmuir* **2013**, *29*, 10566.